Science Advances
AAAS

# Supplementary Materials for

## MAIA, Fc receptor–like 3, supersedes JUNO as IZUMO1 receptor during human fertilization

Jana Vondrakova *et al.*

Corresponding author: Harry Moore, h.d.moore@sheffield.ac.uk;
Katerina Komrskova, katerina.komrskova@ibt.cas.cz

*Sci. Adv.* **8**, eabn0047 (2022)
DOI: 10.1126/sciadv.abn0047

**The PDF file includes:**

Figs. S1 to S10

**Other Supplementary Material for this manuscript includes the following:**

Movies S1 to S10

| | Donor 1 | | | Donor 2 | | | Donor 3 | | | Donor 4 | | | Donor 5 | | |
|---|---|---|---|---|---|---|---|---|---|---|---|---|---|---|---|
| | Exp1 | Exp2 | Exp3 | Exp1 | Exp2 | Exp3 | Exp1 | Exp2 | Exp3 | Exp1 | Exp2 | Exp3 | Exp1 | Exp2 | Exp3 |
| Group | 1,2,3,4 | 1,2,3,4 | 1,2,3,4 | 1,2,3,4 | 1,2,3,4 | 1,2,3,4 | 1,2,3,4 | 1,2,3,4 | 1,2,3,4 | 1,2,3,4 | 1,2,3,4 | 1,2,3,4 | 1,2,3,4 | 1,2,3,4 | 1,2,3,4 |
| Bead | | | | | | | | | | | | | | | |
| 1 | 0,0,1, 0 | 0,0,0,0 | 0,0,2,0 | 0,0,3,0 | 0,0,2,0 | 0,0,0,0 | 0,0,0,5 | 0,0,0,0 | 0,0,2,0 | 0,0,0,0 | 0,0,0,0 | 0,0,0,0 | 0,0,5,1 | 0,0,8,0 | 0,0,2,0 |
| 2 | 0,0, 0,0 | 0,0,0,0 | 0,0,0,0 | 0,0,0,0 | 0,0,0,0 | 0,0,0,0 | 0,0,0,0 | 0,0,0,0 | 0,0,0,0 | 0,0,0,0 | 0,0,0,0 | 0,0,0,0 | 0,0,0,0 | 0,0,0,0 | 0,0,0,0 |
| 3 | 1,0, 5,1 | 2,1,4,0 | 2,0,6,2 | 2,0,2,1 | 1,0,3,0 | 2,,0,7,2 | 1,0,3,0 | 0,0,0,0 | 0,0,0,0 | 1,1,4,2 | 2,1,4,1 | 3,1,4,2 | 3,1,4,2 | 2,2,5,1 | 0,0,4,0 |
| 4 | 0,0, 2,0 | 0,0,4,0 | 1,0,6,2 | 1,0,3,0 | 2,1,5,0 | 1,0,0,0 | 2,0,0,0 | 2,1,4,0 | 0,0,0,0 | 1,0,0,0 | 2,1,0,0 | 1,0,3,0 | 0,0,0,0 | 0,0,0,0 | 0,0,0,0 |
| 5 | 0,0, 0,0 | 0,0,0,0 | sperm v.poor | 0,0,0,0 | 0,0,0,0 | 0,0,0,0 | 0,0,0,0 | 0,0,0,0 | 0,0,0,0 | 0,0,0,0 | 0,0,0,0 | 0,0,0,0 | 0,0,0,0 | 0,0,0,0 | 0,0,0,0 |
| 6 | 0,0, 0,0 | 0,0,3,0 | ,0,0,6,2 | 0,0,0,0 | 0,0,0,0 | 2,1,5,2 | 0,0,0,0 | 0,0,3,0 | 0,0,2,0 | 0,0,5,1 | 2,0,7,2 | 2,1,9,3 | 0,0,6,1 | 4,1,7,2 | 0,0,3,0 |
| 7 | 3,0, 7,0 | 2,0,8,2 | 1,0,2,1 | 0,0,3,0 | 1,0,5,0 | 1,1,0,0 | 2,0,4,0 | 6,1,12,2 | 3,1,6,1, | 0,0,0,0 | 2,1,13,5 | 5,2,9,2 | 0,0,0,0 | 0,0,0,0 | 0,0,0,0 |
| 8 | 0,0, 0,0 | 0,0,0,0 | ,0,0,4,2 | 0,0,0,0 | 0,0,0,0 | 0,0,0,0 | 10,4,26,7 | 12,3,29,3 | 6,2,17,8 | 0,0,0,0 | 0,0,0,0 | 0,0,0,0 | 2,0,0,0 | 2,1,6,2 | 0,0,0,0 |
| 9 | 18,5,31,13 | 14,12,29,18 | 10,6,22,12 | 9,3,16,8 | 22,12,37,6 | 16,9,29,22 | 17,3,25,12 | 16,2,24,9 | 10,7,26,16 | 8,2,17,8 | 21,14,39,23 | 26,14,45,21 | 14,7,19,7 | 23,15,39,25 | 16,7,19,12 |
| 10 | 0,0, 0,0 | 0,0,0,0 | ,0,0,4,1 | 0,0,0,0 | 0,0,0,0 | 0,0,0,0 | 0,0,0,0 | 0,0,0,0 | 0,0,0,0 | 0,0,0,0 | 0,0,0,0 | 0,0,0,0 | 0,0,0,0 | 0,0,0,0 | 0,0,0,0 |
| 11 | 0,0, 0,0 | 0,0,0,0 | ,0,0,6,3 | 0,0,0,0 | 0,0,0,0 | 0,0,0,0 | 0,0,0,0 | 0,0,0,0 | 0,0,0,0 | 0,0,0,0 | 0,0,0,0 | 0,0,0,0 | 0,0,0,0 | 0,0,0,0 | 0,0,0,0 |
| 12 | 0,0, 0,0 | 0,0,0,0 | ,0,0,7,3 | 0,0,0,0 | 0,0,0,0 | 0,0,0,0 | 0,0,0,0 | 0,0,0,0 | 0,0,0,0 | 0,0,0,0 | 0,0,0,0 | 0,0,0,0 | 0,0,0,0 | 0,0,0,0 | 0,0,0,0 |
| 13 | 0,0, 0,0 | 0,0,6,2 | ,0,1,9,3 | 0,2,12,4 | 2,0,2,1 | 0,0,3,0 | 3,1,5,0 | 0,0,2,0 | 2,0,6,0 | 7,2,2,0 | 1,3,5,2 | 4,3,15,2 | 4,1,10,3 | 5,1,14,5 | 9,2,22,6 |
| 14 | 0,0, 0,0 | 0,0,0,0 | ,0,0 | 0,0,0,0 | 0,0,0,0 | 0,0,0,0 | 0,0,0,0 | 0,0,0,0 | 0,0,0,0 | 0,0,0,0 | 0,0,0,0 | 0,0,0,0 | 0,0,0,0 | 0,0,0,0 | 0,0,0,0 |
| 15 | 7,2,8,4 | 12,3,16,4 | 5,2,8,0 | 9,3,22,14 | 11,4,27,12 | 8,4,15,8 | 2,0,4,1 | 0,0,5,1 | 1,0,3,1 | 3,0,9,4 | 1,0,1,0 | 0,0,2,1 | 6,2,19,5 | 3,8,16,4 | 2,1,8,6 |
| 16 | 34, 1, 84,6 | 20, 0, 66, 3 | 41,2, 104, 8 | 12,0,39, 1 | 4,0, 52, 9 | 6,0,74,4 | 54,5,109,12 | 38, 4, 82, 15 | 12,0, 29,3 | 25,3,48,6 | 35,7,65,9 | 43,4,92,10 | 18,1,38, 4 | 26,3,76,7 | 36,3,82,12 |
| 17 | 0,0, 0,0 | 0,0,0,0 | ,0,0,1,0 | 0,0,0,0 | 0,0,0,0 | 0,0,0,0 | 0,0,0,0 | 0,0,0,0 | 0,0,0,0 | 0,0,0,0 | 0,0,0,0 | 0,0,0,0 | 0,0,0,0 | 0,0,0,0 | 0,0,0,0 |
| 18 | 6,0, 0,0 | 3,1,0,0 | 3,3,6,1 | 2,0,12,2 | 4,0,7,1 | 9,4,19,4 | 6,2,12,5 | 4,0,2,0 | 8,3,16,6 | 5,0,8,1 | 6,0,02,3 | 4,1,9,4 | 0,0,8,0 | 3,1,6,2 | 2,0,2,0 |
| 19 | 0,0, 0,0 | 0,0,0,0 | ,0,0 | 0,0,0,0 | 0,0,0,0 | 0,0,0,0 | 2,0,0,0 | 1,0,3,1 | 0,0,2,0 | 3,0,5,2 | 5,2,7,2 | 4,1,6,2 | 0,0,0,0 | 0,0,0,0 | 0,0,0,0 |
| 20 | 14,4,22,10 | 16,7,27,13 | 12,5,19,13 | 1,0,3,0 | 2,1,3,2 | 1,2,5,2 | 0,0,0,0 | 0,0,0,0 | 0,0,0,0 | 3,1,5,6 | 9,3,16,5 | 11,2,19,7 | 0,0,0,0 | 0,0,0,0 | 0,0,0,0 |
| 21 | 0,0, 0,0 | 0,0,0,0 | ,0,0 | 0,0,0,0 | 0,0,0,0 | 0,0,0,0 | 0,0,0,0 | 0,0,0,0 | 0,0,0,0 | 0,0,0,0 | 0,0,0,0 | 0,0,0,0 | 0,0,0,0 | 0,0,0,0 | 0,0,0,0 |
| 22 | 0,0, 2,5 | 5,2,6,3 | 3,6,3,4 | 6,3,6,9, | 3,3,7,12 | 0,1,2,5 | 0,0,3,3 | 0,1,4,3 | 0,2,0,3 | 1,3,7,12 | 2,2,15,17 | 6,5,12,23 | 9,13,22,26 | 12,10,17,15 | 6,4,16,22 |
| 23 | 0,0, 0,0 | 0,0,0,0 | ,0,0 | 0,0,0,0 | 0,0,0,0 | 0,0,0,0 | 0,0,0,0 | 0,0,0,0 | 0,0,0,0 | 0,0,0,0 | 0,0,0,0 | 0,0,0,0 | 0,0,0,0 | 0,0,0,0 | 0,0,0,0 |

**Fig. S1. Sperm-bead binding assay with homologous bead aliquots.** The assay was performed in the presence (group 1 and 3) and absence (group 2 and 4) of calcium for 2 h (group 1 and 2) and 18 h (group 3 and 4) incubation. Mean sperm bound for each condition is shown for 5 sperm donors and triplicate experiments. Beads that consistently bound sperm (yellow) for triplicate experiments. Bead 16 for FcRL3 peptide (brown).

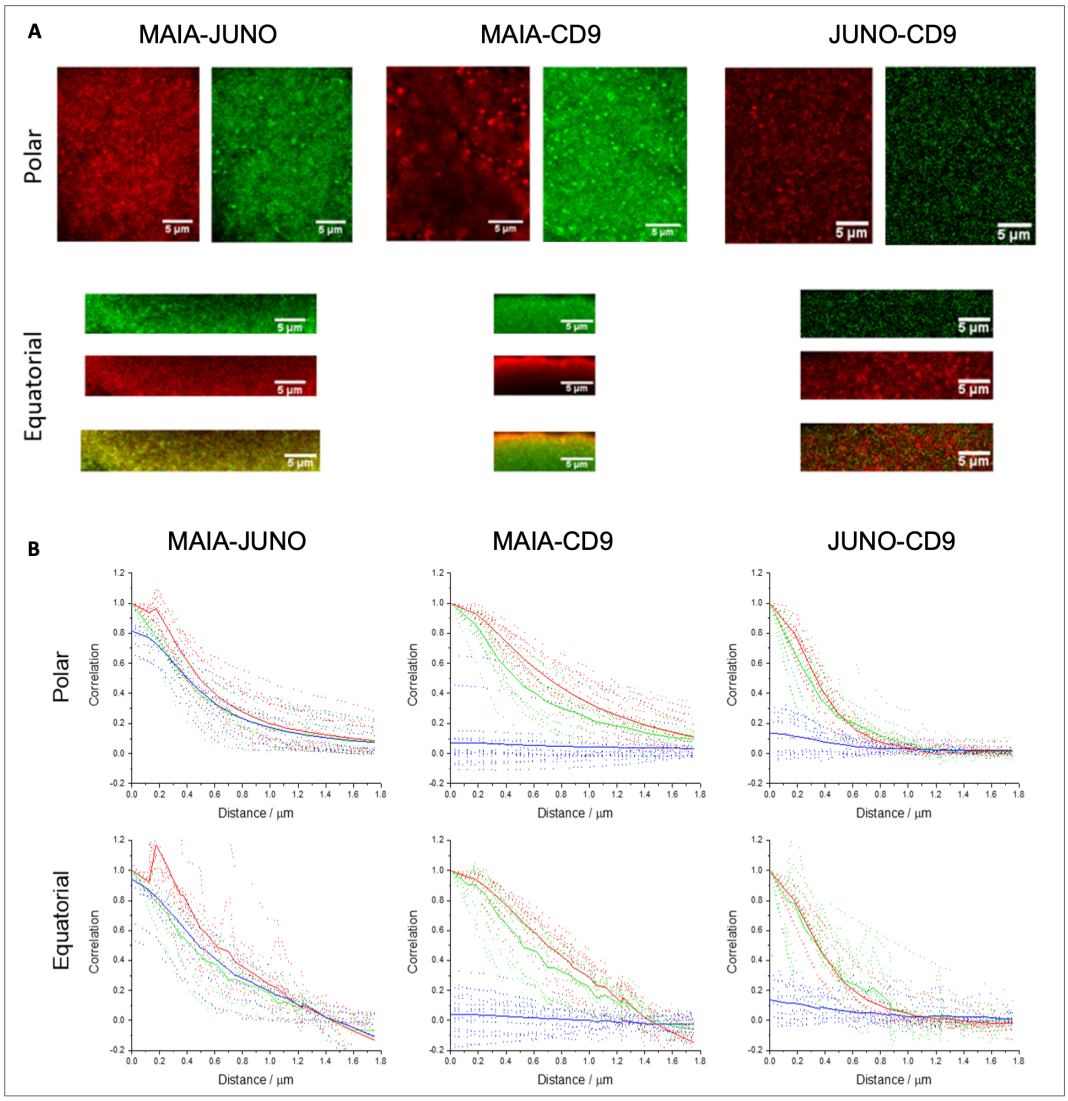


**Fig. S2. Characterisation of local co-localization between MAIA-JUNO, MAIA-CD9 and JUNO-CD9 in unfertilized human oocytes.** (**A**) Co-localization of local intensity variation in two channels (green and red) corresponding to two proteins of interest. Examples of frames from polar and equatorial sub-stacks, overlay for equatorial sub-stacks. Polar sub-stack is approximately a square of 20 µm x 20 µm located close to centre of image and consists of 4 - 10 slices selected near the bottom or the top of stack where cell membrane lies approximately parallel to focal plane within selected region of interest. Equatorial sub-stack consists of 10 - 30 slices containing a cross-section of the membrane close to centre of stack where the membrane is as close as possible to being perpendicular to focal plane. One or two equatorial sub-stacks selected with total area of at least 6 µm x 30 µm. (**B**) Co-localization revealed by intensity of two channels characterised by spatial auto-correlation and cross-correlation functions (ACFs and CCFs) and calculated from polar or equatorial sub-stacks. ACFs and CCFs correlation functions for individual sub-stacks in dotted, their averages are in solid lines. Green and red lines correspond to green and red channel and CCFs plotted as blue lines.

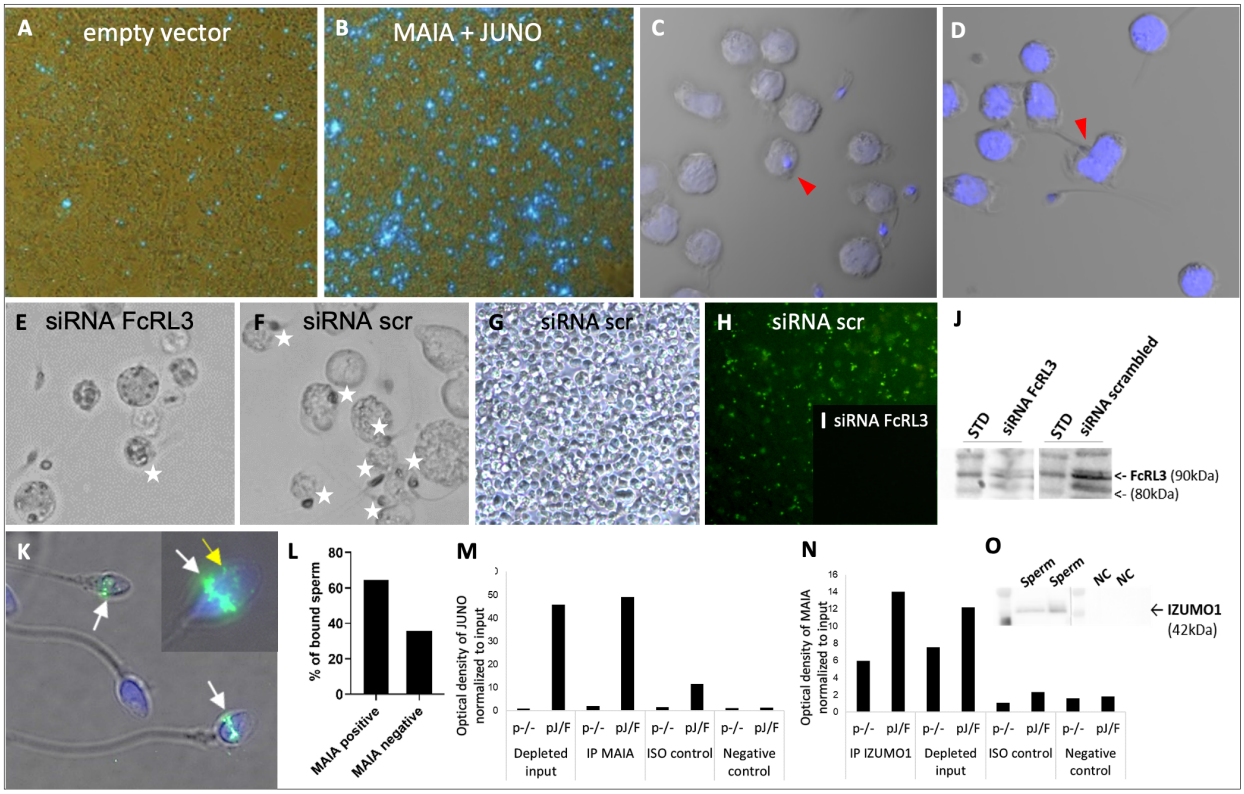


**Fig. S3. Binding and protein interaction detected using human sperm.** (**A** and **B**) Representative immunofluorescent image of attached sperm stained with Hoechst 33342 (blue) binding to MAIA and JUNO co-transfected HEK cells used for ImageXpress quantification analysis. (**C** and **D**) Human JeKo-1 B lymphocytes (JeKo-1) and human sperm were used in binding assays, human sperm (**C**) or JeKo-1 (**D**) were pre-loaded with Hoechst 33342 before binding. Images were captured using a confocal microscope and overlaid with DIC. Red arrows show fusion events (**C** and **D**). (**E** to **J**) Sperm do not bind to JeKo-1 transfected with FcRL3 siRNA (**E**) compares to control JeKo-1 with scrambled siRNA-GFP (scr) (**F**); JeKo-1 transfected with siRNA-GFP scr brightfield-GFP merged (**G**), GFP signal (**H**), FcRL3 JeKo-1 knock-down using FcRL3-siRNA (bottom right corner) (**I**); Efficiency of siRNA knock-down assessed by western blot (**J**). (**K**) Soluble extracellular domain of FcRL3/MAIA binds to IZUMO1, which is localised in the sperm head equatorial segment (ES, white arrow) and inner acrosomal membrane (IAM, yellow arrow), after the acrosome reaction, see detail (top right corner) detected by His-tag labelling. (**L**) Percentage of sperm bound to soluble extracellular domain of FcRL3/MAIA (MAIA positive) and sperm not labelled for presence of peptide (MAIA negative). (**M** and **N**) Optical density analysis of Co-IP experiment (see Fig. 5B and C); JUNO for MAIA - JUNO Co-IP protein complex detected by western blot (**M**); Optical density of MAIA for MAIA - IZUMO1 Co-IP protein complex detected by western blot (**N**); analysis carried out by ImageJ/Fiji software (**M, N**). (**O**) Control detection of IZUMO1 in human sperm (n = 2) (see Fig. 5C), NC (negative control), (n = 2).

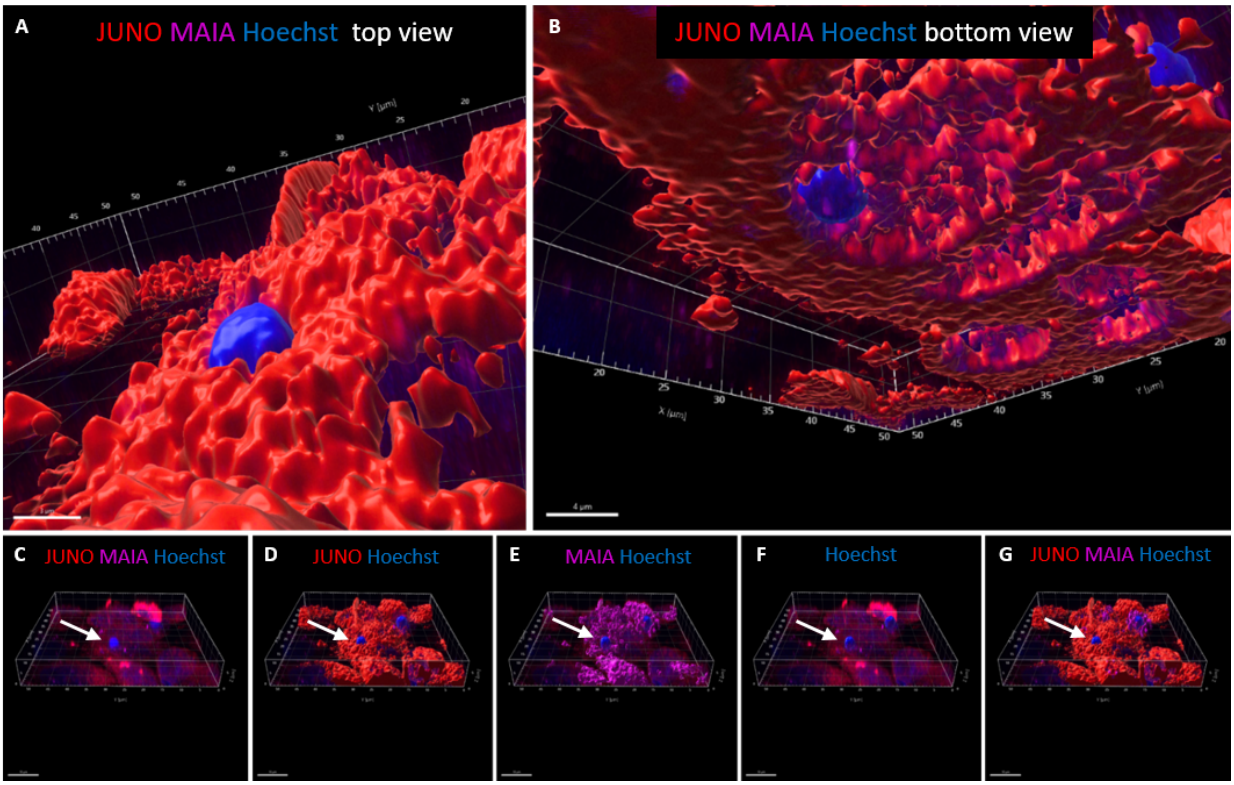


**Fig. S4. Surface Render analysis of fused human sperm with CHO cell.** (**A** and **B**) Surface Render analysis of CHO cell expressing recombinant JUNO (red) and FcRL3 (magenta) demonstrating sperm-CHO penetration and fusion performed by Microscopy image analysis software Imaris, (**A**) top view, (**B**) bottom view, (see movie S4). (**C**) Confocal image (maximal intensity projection) of fused sperm (arrow) with CHO cell, JUNO (red), MAIA (magenta), nuclei stained with Hoechst 33342 (blue). (**D** to **G**) Surface Render analysis of (**D**) JUNO and fused sperm (arrow), (**E**) MAIA and fused sperm (arrow), (**F**) nuclei (Hoechst), (**G**) JUNO, MAIA and fused sperm head (arrow).

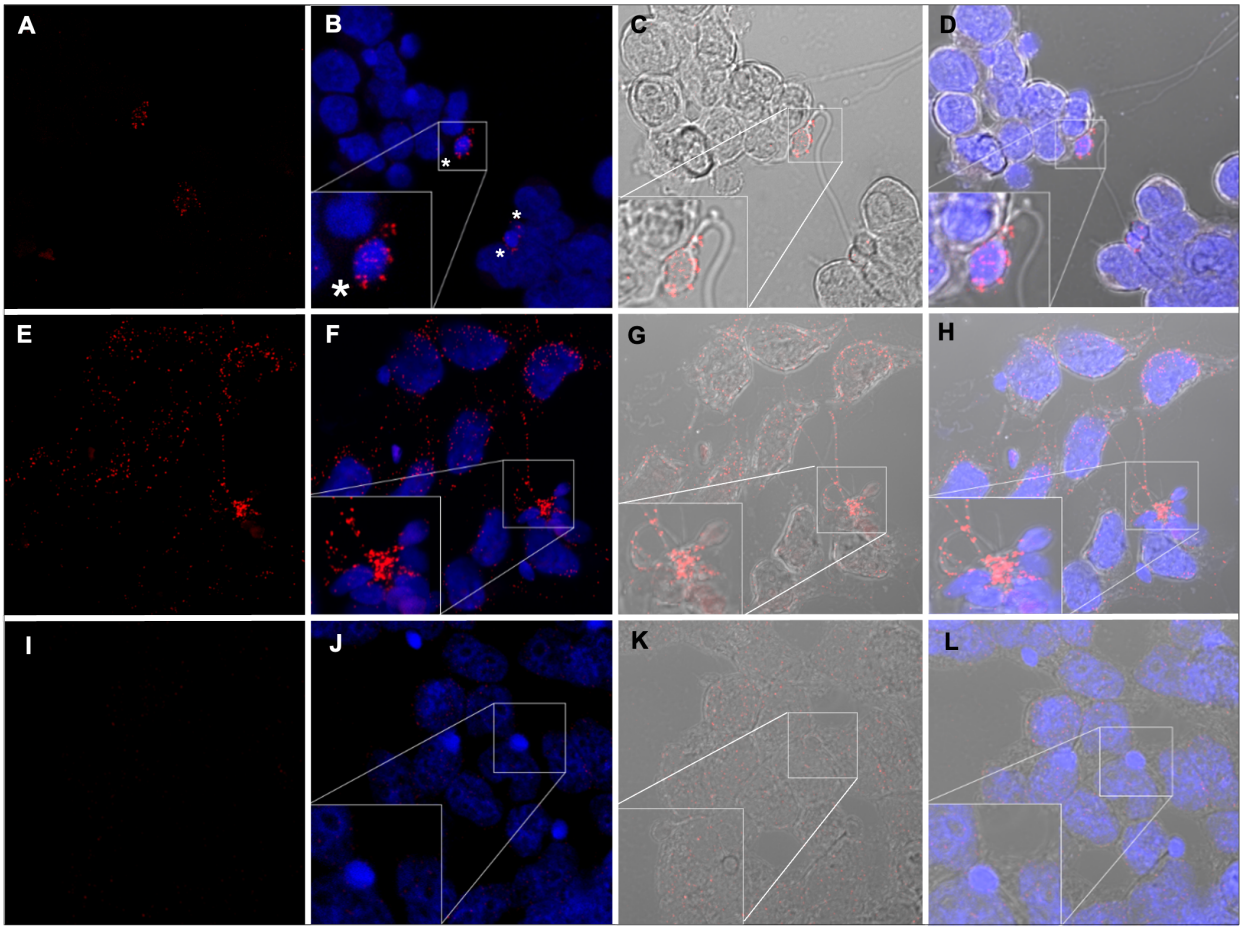


**Fig. S5. MAIA - IZUMO1 interaction using transfected cells and human sperm detected by PLA. (A** to **D)** PLA showing close proximity of protein pairs of MAIA - IZUMO1 in JUNO + FcRL3 double transfected HEK cells with sperm; white asterisks. (**E** to **H)** PLA assay positive control (PC) α-tubulin - β-tubulin. (**I** to **L)** PLA assay negative control (NC) MAIA - β-tubulin. Separated channels for each colour: (**A, E, I**) red, (**B, F, J**) red + blue, (**C, G, K**) DIC + red, (**D, H, L**) merged; details in bottom left corners.

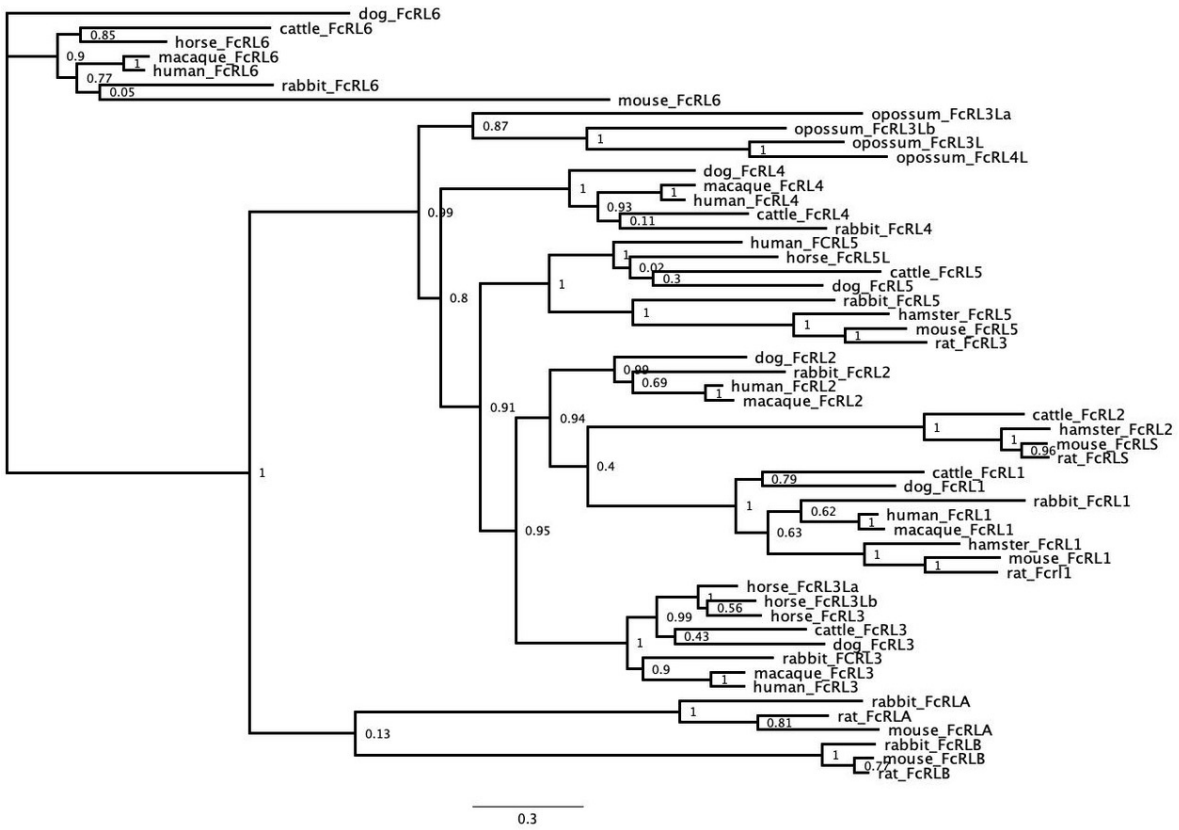


**Fig. S6. Phylogeny of the *FcRL* gene family.** A gene phylogeny was inferred using the translated amino acid sequences of *FcRL* genes in mammals. Major annotated clades of *FcRL* were supported by high branch support probabilities (approximate Likelihood Ratio Tests (aLRT)) as indicated to the right of each node. Most notably for this study, the *FcRL3* gene clade is highly supported (P=0.98) to the exclusion of the closely related paralogs *FcRL1* and *FcRL5*. *FcRL1* and *FcRL3* were both lost in murine and cricetid rodents, but *FcRL5* was maintained in mice, rats, and hamsters. Phylogeny was constructed by PhyML (see Methods).

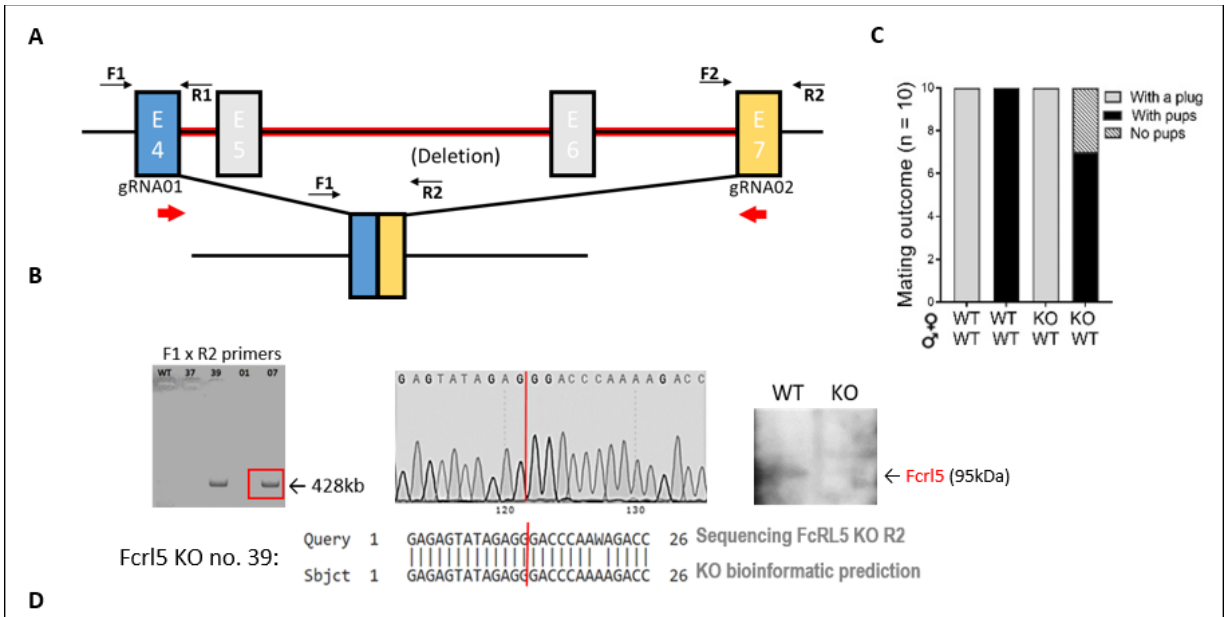


| Fertility success rate | | | | | | | | | Pups data collection related to no. of matings | | | | |
|---|---|---|---|---|---|---|---|---|---|---|---|---|---|
| Genotype of females | Total number of females | No. of females with a vaginal plug | No. of females with fertilization output | No. of females with unsuccessful fertilization | Average unsuccessful fertilization [%] | No. of matings | No. of litters | Average successful mating [%] | Born | Average litter size ±SD | Average preweaning loss ±SD | Average number of pups weaned ±SD | Sex ratio (M/F) |
| WT | 11 | 11 | 11 | 0 | 0.00 | 22 | 22 | 100 | 166 | 8 ±2.405 | 1 ±1.406 | 7 ±3.086 | 1.35 |
| HET | 11 | 11 | 10 | 1 | 9.09 | 15 | 14 | 93 | 103 | 7 ±3.357 | 0 ±0 | 7 ±3.357 | 0.78 |
| KO | 14 | 14 | 13 | 3 | 21.43 | 20 | 17 | 85 | 130 | 7 ±3.472 | 0 ±0.816 | 6 ±3.401 | 1.05 |

**Fig. S7. Genotyping and characterization of *Fcrl5* knock-out mouse model.** (**A**) The schematic representation of the *Fcrl5* gene shows the deleted sequence between its exon 4 and exon7 (E4-E7). Bioinformatic prediction of *Fcrl5*$^{-/-}$ (KO) allele (Query) and allele sequencing result (Subject). (**B**) Genotyping of a Fcrl5$^{-/-}$ mouse: genomic DNA extracted from tail clipping was genotyped by PCR using primer F1xR2 (to check KO); WT - *Fcrl5*$^{+/+}$; PCR products were run on a 2% agarose gel, and examinations and photos were acquired under a UV light trans-illumination; the uncovered Fcrl5 KO product (no. 39) was assessed by Sanger sequencing for determining the sequence of DNA within the splice site, mouse spleen samples. (**C**) Result of *in vivo* mating outcome of *Fcrl5*$^{-/-}$ (KO) female and *Fcrl5*$^{+/+}$ (WT) male mice of breeding pairs (n = 10) show 30% KO/WT pairs after mating without fertilization output, based on a presence of a vaginal plug; (**D**) Summary of fertility success rate and pups data collection; error bars denote standard deviation (SD).

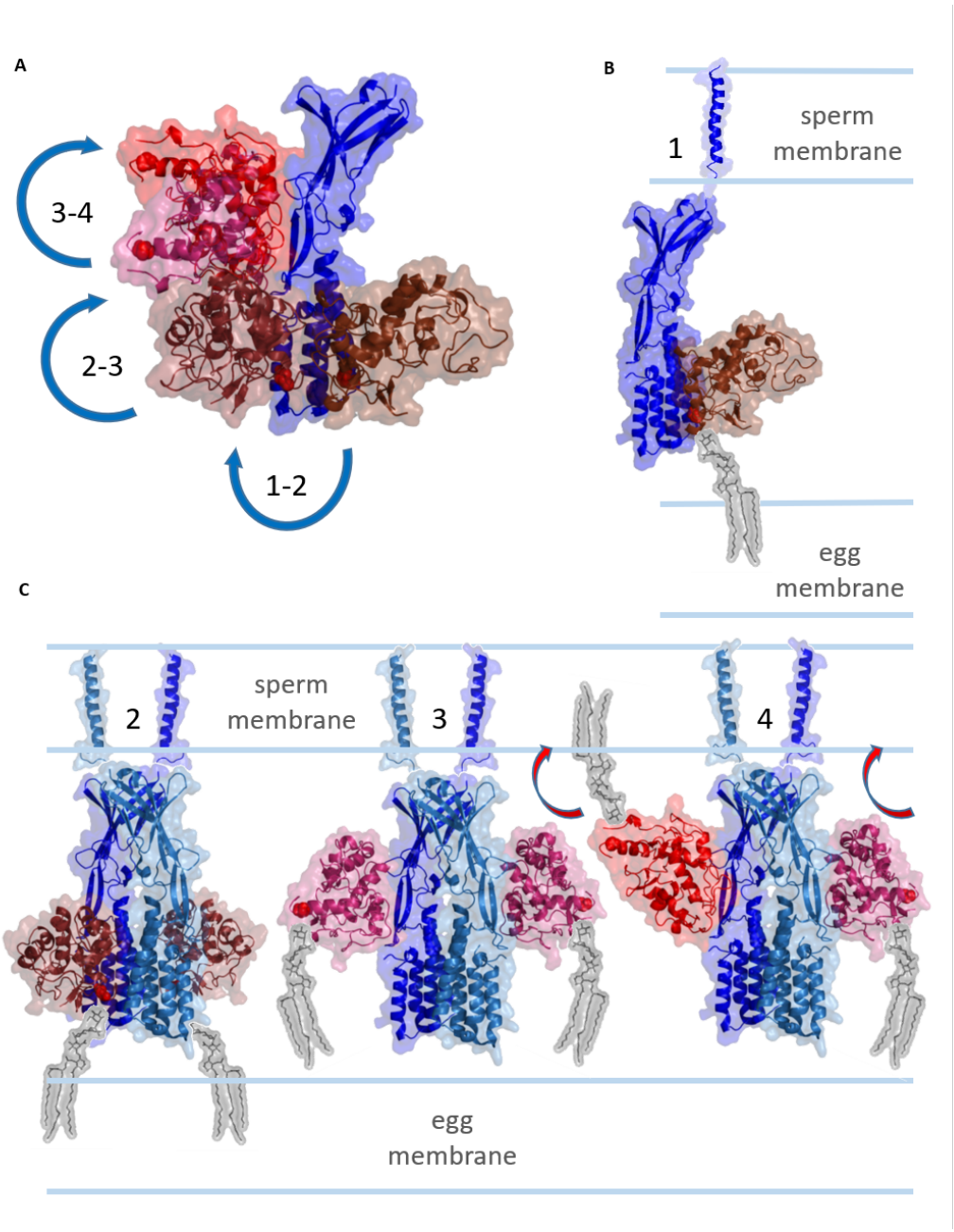


**Fig. S8. Outline of JUNO/IZUMO1 recognition and interaction.** (**A**) JUNO docking to IZUMO1 (blue). Positions of JUNO with increasing affinity are shown in brown to red colour, with the most stable (red) being identical to the crystal structure. Based on the docking data, two possible mechanisms can be suggested: (**B**) The IZUMO1 monomer recognizes single JUNO (**B1**) followed by binding of second IZUMO1. (**C**) A dimer of IZUMO1 is formed initially (blue/light blue), which competes with the B1 interaction site. For both mechanisms, JUNO driven by increasing binding affinity detaches from the egg membrane and relocates to the sperm membrane (**C2** to **C4**) to reach the biologically and crystallographically relevant orientation - JUNO/IZUMO1 2:2 complex anchored in the sperm membrane.

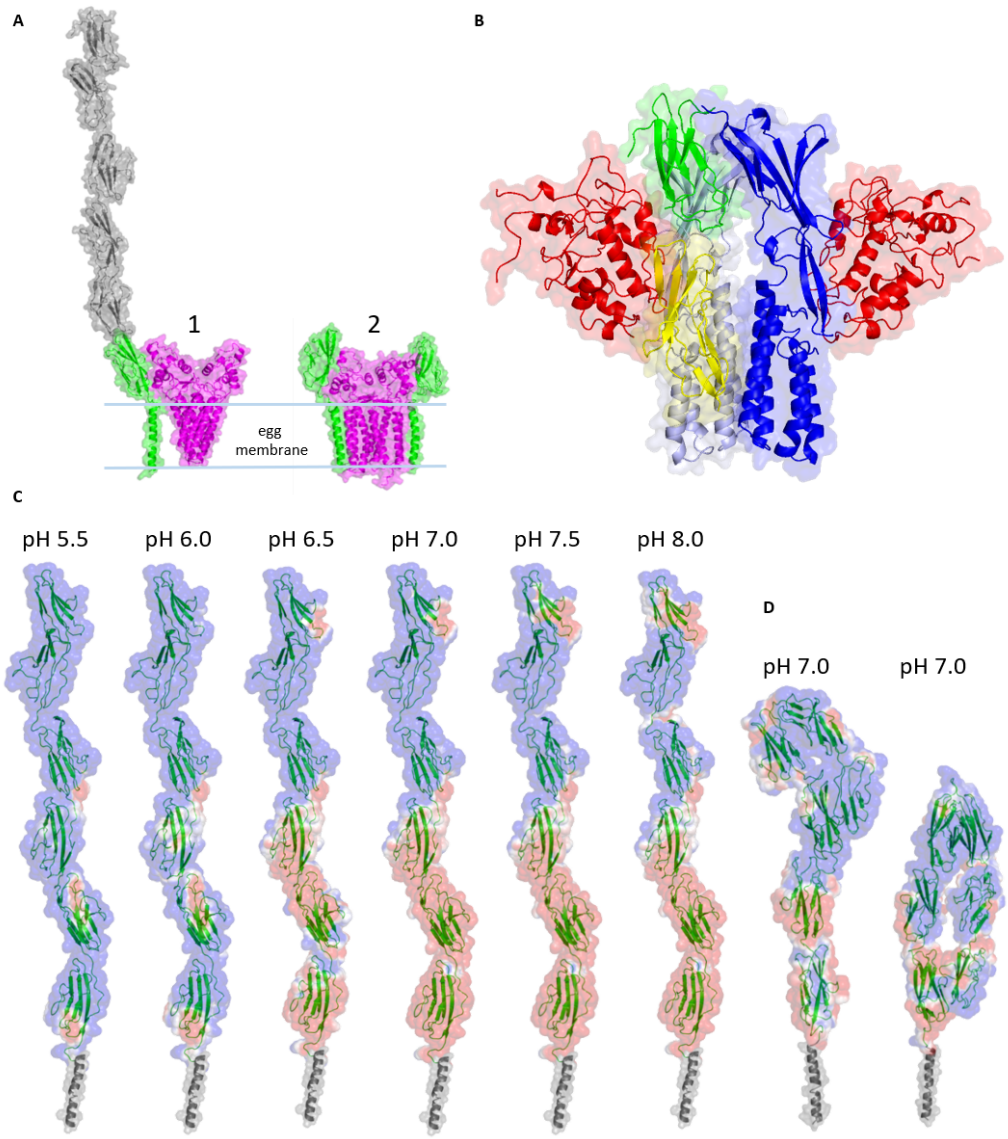


**Fig. S9. Structural analysis of MAIA with CD9 and pH dependency.** (**A1**) Docking prediction of CD9 (magenta, overlayed with a question mark in Fig. **6C** and **D**) dimer formation and interaction with domain 6 of MAIA (green). The remaining domains 1-5 not used in this docking are shown in grey; (**A2**) The 2:2 CD9:MAIA complex after molecular dynamics simulation in an implicit membrane environment. (**B**) Interaction of the 2:2 JUNO/IZUMO1 (red/blue) complex with isolated extracellular domains of MAIA. All MAIA domains were predicted to occupy a common JUNO/IZUMO1 binding interface. The position of domain 1 (green) and domain 2 (yellow) in the JUNO/IZUMO1 groove is shown as an example. (**C**) Obvious pH dependence of FcRL3 partial charges displayed as electrostatic potential (red negative, blue positive) supports the extended conformation at pH<7 while bending, and interaction of the domains is induced at pH>7. (**D**) Alternating patches of negative/positive charge stabilize the bent conformations of MAIA around neutral pH.

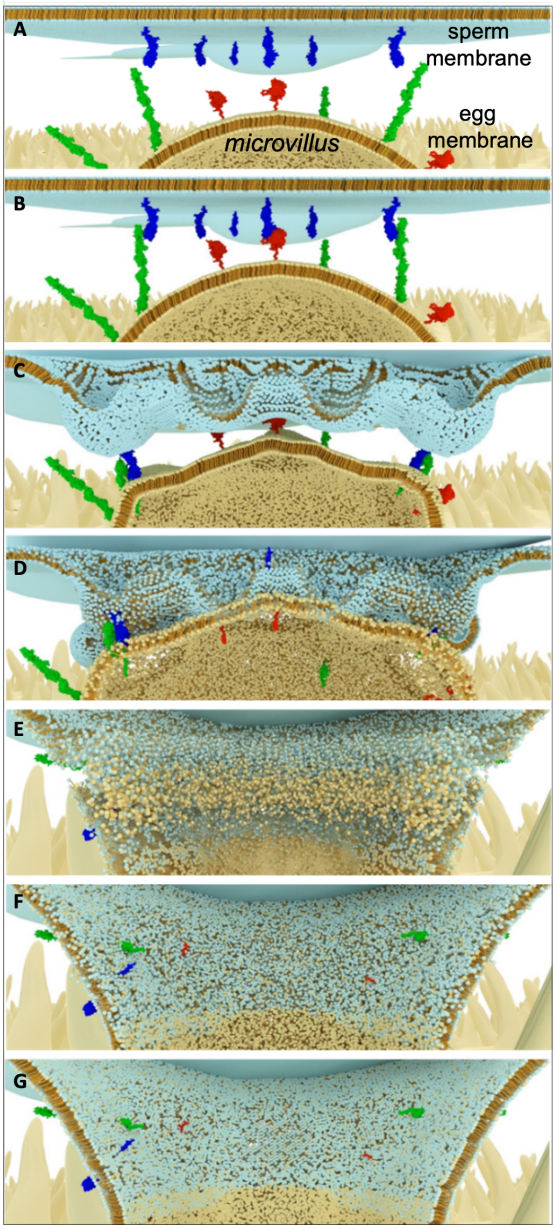


**Fig. S10. Sperm-egg *microvillus* membrane interaction model.** (**A**) Sperm membrane (blue) and egg *microvillus* apex (yellow) in close proximity during sperm attachment to the oolema. (**B**) Apical sperm IZUMO1 (blue) and egg JUNO (red); apico-lateral IZUMO1 and MAIA (green) protein interaction. (**C**) Sperm/egg membrane budding mediated by the close apical IZUMO1-JUNO membrane interaction and active apico-lateral proximisation facilitated by IZUMO1-MAIA protein complex contraction. (**D**) Sperm-egg membrane destabilisation by proximity and hybridisation. The hybridisation surface enlarged and hybridisation facilitated by combined apical (JUNO-IZUMO1) and apico-lateral (MAIA-IZUMO1) interaction. (**E**) Hypothetical representation of membrane destabilisation peak. (**F**) Formation and stabilisation of sperm/egg hybrid membrane. (**G**) Fully developed sperm/egg *microvillus* hybridisation cone.